Supplementary Information

Experimental charge density of organic nanocrystals revealed by 3D electron diffraction

Anil Kumar[a], Ashwin Suresh[b], Arianna Lanza[c], Jakub Wojciechowski[d], Damian Trzybiński[a], Petr Brazda[b], Lukas Palatinus[b*] & Paulina Maria Dominiak[a]*

[a]University of Warsaw, Faculty of Chemistry, Biological and Chemical Research Centre, ul. Żwirki i Wigury 101, 02-089 Warszawa, Poland, [b]Institute of Physics of the Czech Academy of Sciences, Prague, Czech Republic, [c]Department of Chemistry, University of Copenhagen, Universitetsparken 5, 2100 Copenhagen Ø, Denmark, [d]Rigaku Europe SE, Hugenottenallee 167, 63263 Neu-Isenburg, Germany.

This file includes:

Supplementary Materials and Methods
Supplementary Tables S1 to S16
Supplementary Figures S1 to S16
Supplementary references

Supplementary Materials and Methods

Crystallization of L-Tyrosine: To obtain crystals of L-tyrosine, first the L-tyrosine was dissolved in 2M potassium hydroxide (KOH) until a saturated solution was obtained. After that the saturated solution was diluted 1.5× by adding water dilution. The good quality crystals were obtained by slow evaporation of the diluted solution at room temperature.

X-ray Diffraction Data Collection and Structure Refinement of L-Tyrosine: A high-quality single crystal of the investigated compound was selected for diffraction experiments conducted at T = 100(2) K. High-resolution X-ray diffraction data were collected using an Agilent Technologies SuperNova Dual Source diffractometer, equipped with a micro-focus Mo(K_α) X-ray tube and a HyPix 6000HE hybrid pixel array detector. The crystal-to-detector distance was maintained at 55 mm. Data collection up to a resolution of 0.43 Å (with an omega scan width of 0.5 °) required 77 hours, 33 minutes, and 38 seconds. The data reduction was performed using CrysAlisPro. The reflections were merged using SORTAV[1] implemented in the WINGX program[2]. The structure solution and IAM structure refinement were performed using SHELXT[3] and Olex2 programs implemented in the OLEX2 suite[4]. All non-hydrogen atoms were refined anisotropically, and hydrogens coordinates and displacement parameter were derived with a riding model.

Computational Methods Section

Geometry optimization: To obtain the theoretical structure factors, firstly the experimental geometry (atomic coordinates) of L-alanine, urea and L-Tyrosine was optimized with frozen unit cell parameters by applying periodic DFT calculations using *CRYSTAL17*[5]. All the calculations were carried out with the B3LYP functional[6] and the POB-TZVP basis set[7]. The B3LYP was augmented with an empirical dispersion term as proposed by Grimme[8] and modified for molecular crystals[6]. A full, simultaneous relaxation of atomic coordinates by means of analytical energy gradients was applied. The level of accuracy in evaluating the Coulomb and exchange series was controlled by five TOLINTEG parameters for which values of 10^{-6} , 10^{-6} , 10^{-6} , 10^{-7}, 10^{-29} were used. The DFT exchange-correlation contribution was evaluated by numerical integration over the cell volume. Radial and angular points of the atomic grid were generated through Gauss−Legendre and Lebedev quadrature schemes. The condition for the self-consistent field (SCF) convergence was set to 10^{-7} on the total energy difference between two subsequent cycles. The shrinking factors

(IS) along the reciprocal lattice vectors were set at 4. The level shifter value was set to 0.6 Hartree. Upon energy convergence the periodic wave function was obtained.

Theoretical electron diffraction data: The X-ray static structure factors (no thermal motion included, i.e ADPs were set to zero) were computed through the dedicated module of CRYSTAL17 from the wave function file (.f9 file) obtained after the geometry optimization step and the set of hkl indices (.d3 file). The sets of hkl indices for L-alanine, urea and L-tyrosine were generated up to resolution d_{min} = 0.44, 0.53 and 0.59 Å respectively, by the *XD* software using the *XDHKL* module[9].

Theoretical electron static structure factors were computed from theoretical X-ray static structure factors by application of the Mott-Bethe formulae[10] using dedicated *DiSCaMB* utility program[11]. The theoretical structure factors represented perfect, error-free values with constant small values of $\sigma(F)$ and are exempted from dynamic diffraction effects.

Table S1. Summary of the data collection, reduction and kinematical refinement of the three compounds.

Parameters	L-alanine	Urea	L-tyrosine
	Data collection		
Chemical formula	$C_3H_7NO_2$	CH_4N_2O	$C_9H_{11}NO_3$
Formula weight (g mol^{-1})	89.09	60.06	181.2
Tilt range, tilt step (°)	-52 to +59, 0.15	-63 to +60, 0.2	-55 to +30, 0.3
Exposure time per frame (s)	0.3	0.6	0.4
Flux density (e s^{-1} Å^{-2})	0.01	0.003	0.005
Total fluence (e Å^{-2})	2.3	1.10	0.6
Detector distance (mm)	472.02	479.00	319.00
Temperature (K)	100	100	95
	Data reduction		
Space group	$P2_12_12_1$	$P\text{-}42_1m$	$P2_12_12_1$
Unit cell *a*, *b*, *c* (Å)	5.7691(4), 5.9494(4), 12.2453(7)	5.6308(4), 5.6308(4), 4.7145(10)	5.8355, 6.8686, 21.1363
Angles α, β, γ (°)	90.0, 90.0, 90.0	90.0, 90.0, 90.0	90.0, 90.0, 90.0
Volume (Å^3)	420.29(4)	149.48(3)	847.18
Resolution full/last shell (Å)	0.44/0.47-0.44	0.53/0.56-0.53	0.59/0.63-0.59
Completeness full/ last shell resolution (%)	99/99.1	95.5/98	90.3/93.2
Redundancy full/ last shell resolution	3.66/3.2	7.11/6.96	3.5/3.67
$I/\sigma(I)$ (count) full/ last shell resolution	19.82/1.05	12.86/0.81	18.68/3.17
$I/\sigma(I)$ (error model) full/ last shell resolution	3.68/1.09	3.96/0.71	3.78/1.55
R_{int} obs full/ last shell resolution (%)	12.51/16.42	16.26/19.12	13.43/12.06
R_{int} all full/ last shell resolution (%)	16.38/61.14	19.02/64.15	16.67/39.32
$CC_{1/2}$ full/ last shell resolution (%)	98.78/28.3	98.69/79.93	97.08/59.97
Total reflections	10353	2404	7994
Unique reflections	5026	587	2288
	Kinematical refinement		
Reflections used [$I > 3\sigma(I)$]/all	2508/5026	294/587	2140/3999
Constraints/Restraints/Parameters	0/0/83	0/0/21	0/0/163
R_1 [$I > 3\sigma(I)$]/ all (%)	17.18/20.02	18.37/20.85	15.20/18.56
wR_1 [$I > 3\sigma(I)$]/ all (%)	23.32/24.82	23.56/24.17	21.61/23.67
$GooF_{obs/all}$	2.46/1.93	3.37/2.46	2.29/1.91
Residual potential Max./min. (e Å^{-1})	1.33/-1.90	0.90/-2.22	0.76/-0.76

Table S2. Root-mean-square difference (RMSD) for X–H bond lengths (Å), charges (e): based on P_{val}, κ, κ', ρ_{bcp} (e Å^{-3}): electron density and $\nabla^2\rho_{bcp}$ (e Å^{-5}): Laplacian at the BCP of the covalent bond and intermolecular interaction (H···Acceptor) of L-alanine.

RMSD		eMM_{exp} vs eMM_{theo}	eMM_{exp} vs xMM_{exp}	xMM_{exp} vs eMM_{theo}	eMM_{exp} vs $eIAM_{exp}$
X–H bond lengths		0.013	0.011	0.006	0.04
Charges	All atoms (except N1 & C2)	0.14	0.10	0.14	
	Non-H atoms (except N1 & C2)	0.08	0.12	0.16	
	H-atoms	0.17	0.08	0.12	
κ	All atoms	0.07	0.07	0.06	
	Non-H atoms	0.05	0.03	0.04	
	H-atoms	0.09	0.10	0.09	
κ'	All atoms	0.12	0.12	0.09	
	Non-H atoms	0.13	0.13	0.09	
	H-atoms	0.09	0.08	0.10	
ρ_{bcp} (Covalent bond)	All atoms	0.18	0.19	0.10	
	Non-H atoms	0.24	0.17	0.09	
	H-atoms	0.12	0.20	0.11	
$\nabla^2\rho_{bcp}$ (Covalent bond)	All atoms	6.25	7.64	4.04	
	Non-H atoms	7.68	5.54	2.53	
	H-atoms	5.00	8.84	4.83	
ρ_{bcp} (H···Acceptor)		0.03	0.04	0.04	
$\nabla^2\rho_{bcp}$ (H···Acceptor)		0.30	0.36	0.42	

Table S3. Electrostatic potential surface quantities (Bohr Å^{-1}) of L-alanine.

	$V_{s\ av.}^{+}$	$V_{s\ av.}^{-}$	Π
eMM_{exp}	0.245	-0.047	0.135
eMM_{theo}	0.234	-0.057	0.126
xMM_{exp}	0.211	-0.077	0.149

$\mathbf{V_s^+}_{\mathbf{av.}}$ -Average of positive surface values; $\mathbf{V_s^-}_{\mathbf{av.}}$ - Average of negative surface value

Π - Average deviation from the average surface value;

Table S4. Topological parameters of the covalent bonds of L-alanine.

Rij: BP length; d_1, d_2: distances between the BCP and each bonded atom, ρ_{bcp}: electron density and $\nabla^2\rho_{bcp}$: Laplacian at the BCP. For each covalent bond, the first, second and third lines refers to the eMM_{exp}, eMM_{theo} and xMM_{exp} models, respectively.

Bonds	*Rij* (Å)	d_1 (Å)	d_2 (Å)	ρ_{bcp} (e Å^{-3})	$\nabla^2\rho_{bcp}$ (e Å^{-5})
O1-C1	1.255	0.838	0.417	2.818	-35.850
	1.273	0.799	0.474	2.468	-26.875
	1.268	0.830	0.438	2.616	-30.438
O2-C1	1.242	0.830	0.412	2.843	-32.581
	1.253	0.817	0.436	2.577	-22.094
	1.251	0.829	0.421	2.677	-23.841
N1-C2	1.482	0.957	0.524	1.578	-11.978
	1.497	0.815	0.682	1.588	-5.566
	1.492	0.843	0.649	1.647	-9.055
C1-C2	1.527	0.797	0.730	1.975	-19.175
	1.530	0.755	0.775	1.686	-11.290
	1.538	0.762	0.776	1.742	-13.126
C2-C3	1.520	0.773	0.747	1.487	-7.823
	1.525	0.764	0.761	1.588	-8.701
	1.529	0.775	0.754	1.602	-9.478
N1-H2	1.036	0.817	0.219	2.082	-43.487
	1.034	0.783	0.252	2.143	-41.704
	1.040	0.758	0.282	2.234	-36.430
N1-H3	1.046	0.817	0.229	2.071	-40.667
	1.047	0.796	0.251	2.073	-41.045
	1.040	0.757	0.283	2.218	-34.906
N1-H4	1.035	0.856	0.179	1.910	-52.865
	1.039	0.787	0.252	2.113	-40.862
	1.040	0.764	0.276	2.151	-34.136
C2-H1	1.087	0.671	0.416	1.736	-15.198
	1.089	0.684	0.405	1.889	-19.698
	1.099	0.682	0.417	1.962	-21.910
C3-H5	1.085	0.684	0.400	1.702	-15.341
	1.091	0.700	0.391	1.821	-17.759
	1.084	0.688	0.396	1.930	-20.757
C3-H6	1.066	0.673	0.393	1.746	-16.529
	1.090	0.701	0.389	1.784	-16.298
	1.084	0.686	0.398	1.976	-22.489
C3-H7	1.067	0.686	0.381	1.711	-16.649
	1.090	0.697	0.393	1.833	-17.758
	1.084	0.698	0.385	1.843	-18.494

Table S5. Topological parameters of intermolecular interactions of L-alanine.

Rij: BP length; d_1, d_2: distances between the BCP and each bonded atom, ρ_{bcp}: electron density and $\nabla^2\rho_{bcp}$: Laplacian at the BCP. For each covalent bond, the first, second and third lines refers to the eMM_{exp}, eMM_{theo} and xMM_{exp} models, respectively.

Interactions	Symmetry codes	*Rij* (Å)	d_1 (Å)	d_2 (Å)	ρ_{bcp} (e Å^{-3})	$\nabla^2\rho_{bcp}$ (e Å^{-5})
O1···H3	65501	1.760	1.133	0.627	0.328	1.791
		1.747	1.148	0.599	0.326	1.376
		1.777	1.176	0.601	0.256	2.217
O1···H4	64603	1.817	1.180	0.637	0.263	1.398
		1.784	1.176	0.609	0.261	1.860
		1.817	1.183	0.634	0.226	1.910
O2···H1	65603	2.409	1.473	0.936	0.086	1.070
		2.414	1.441	0.973	0.080	0.832
		2.399	1.469	0.930	0.073	0.829
O2···H2	56604	1.843	1.172	0.671	0.275	1.668
		1.838	1.191	0.647	0.218	1.643
		1.841	1.167	0.674	0.257	1.285
O2···H6	56501	2.743	1.603	1.140	0.034	0.447
		2.661	1.560	1.101	0.035	0.541
		2.700	1.534	1.166	0.046	0.353

Table S6. Root-mean-square difference (RMSD) for X–H bond lengths (Å), charges (e): based on P_{val}, κ, κ', ρ_{bcp} (e Å^{-3}): electron density and $\nabla^2\rho_{bcp}$ (e Å^{-5}): Laplacian at the BCP of the covalent bond and intermolecular interaction (H···Acceptor) of urea.

RMSD		eMM_{exp} vs eMM_{theo}	eMM_{exp} vs xMM_{exp}	xMM_{exp} vs eMM_{theo}	eMM_{exp} vs $eIAM_{exp}$
X-H bond lengths		0.04	0.03	0.003	0.09
Charges	All atoms	0.21	0.16	0.07	
	Non-H atoms	0.21	0.18	0.06	
	H-atoms	0.20	0.14	0.07	
κ	All atoms	0.04	0.01	0.04	
	Non-H atoms	0.01	0.02	0.01	
	H-atoms	0.07	0.002	0.06	
κ'	All atoms	0.14	0.21	0.16	
	Non-H atoms	0.13	0.22	0.18	
	H-atoms	0.17	0.17	0.00	
ρ_{bcp} (Covalent bond)	All atoms	0.32	0.42	0.26	
	Non-H atoms	0.18	0.51	0.34	
	H-atoms	0.41	0.31	0.14	
$\nabla^2\rho_{bcp}$ (Covalent bond)	All atoms	28.36	30.82	7.71	
	Non-H atoms	10.56	19.08	11.90	
	H-atoms	38.69	39.18	0.49	
ρ_{bcp} (H···Acceptor)		0.03	0.04	0.01	
$\nabla^2\rho_{bcp}$ (H···Acceptor)		1.72	1.42	0.32	

Table S7. Electrostatic potential surface quantities (Bohr Å^{-1}) of urea

	$V_{s\ av.}^{+}$	$V_{s\ av.}^{-}$	Π
eMM_{exp}	0.200	-0.132	0.164
eMM_{theo}	0.196	-0.056	0.107
xMM_{exp}	0.176	-0.056	0.109

Table S8: Topological parameters of the covalent bonds of urea.

Rij: BP length; d_1, d_2: distances between the BCP and each bonded atom, ρ_{bcp}: electron density and $\nabla^2\rho_{bcp}$: Laplacian at the BCP. For each covalent bond, the first, second and third lines refers to the eMM_{exp}, eMM_{theo} and xMM_{exp} models, respectively.

Bonds	*Rij* (Å)	d_1 (Å)	d_2 (Å)	ρ_{bcp} (e Å^{-3})	$\nabla^2\rho_{bcp}$ (e Å^{-5})
O1-C1	1.275	0.747	0.528	2.164	-11.952
	1.270	0.810	0.460	2.379	-20.805
	1.257	0.753	0.504	2.822	-36.216
N1-C1	1.362	0.866	0.496	2.064	-8.566
	1.347	0.802	0.545	2.195	-20.588
	1.343	0.763	0.580	2.364	-20.374
N1-H1	0.998	0.822	0.176	2.496	-69.554
	1.013	0.761	0.251	2.180	-35.619
	1.009	0.741	0.268	2.360	-35.151
N1-H2	0.964	0.798	0.167	2.701	-78.752
	1.012	0.758	0.254	2.207	-35.836
	1.009	0.750	0.259	2.278	-35.317

Table S9. Topological parameters of intermolecular interactions of urea.

Rij: BP length; d_1, d_2: distances between the BCP and each bonded atom, ρ_{bcp}: electron density and $\nabla^2\rho_{bcp}$: Laplacian at the BCP. For each covalent bond, the first, second and third lines refers to the eMM_{exp}, eMM_{theo} and xMM_{exp} models, respectively.

Interactions	Symmetry codes	*Rij* (Å)	d_1 (Å)	d_2 (Å)	ρ_{bcp} (e Å^{-3})	$\nabla^2\rho_{bcp}$ (e Å^{-5})
O1···H1		2.055	1.262	0.793	0.293	0.932
		2.009	1.256	0.753	0.253	2.950
		2.006	1.236	0.770	0.241	2.670
O1···H2		2.140	1.295	0.845	0.235	1.666
		2.047	1.244	0.803	0.236	3.016
		2.056	1.246	0.811	0.239	2.663

Table S10. Root-mean-square difference (RMSD) for X-H bond lengths (Å), charges (e): based on P_{val}, κ, κ', ρ_{bcp}(e Å^{-3}): electron density and $\nabla^2\rho_{bcp}$ (e Å^{-5}): Laplacian at the BCP of the covalent bond and intermolecular interaction (H···Acceptor) of L-tyrosine.

RMSD		eMM_{exp} vs eMM_{theo}	eMM_{exp} vs xMM_{exp}	xMM_{exp} vs eMM_{theo}	eMM_{exp} vs $eIAM_{dyn}$
X–H bond lengths		0.02	0.02	0.01	0.04
Charges	All atoms	0.21	0.21	0.17	
	Non-H atoms	0.24	0.23	0.19	
	H-atoms	0.16	0.19	0.13	
κ	All atoms	0.03	0.04	0.05	
	Non-H atoms	0.02	0.02	0.02	
	H-atoms	0.04	0.07	0.09	
κ'	All atoms	0.12	0.17	0.10	
	Non-H atoms	0.11	0.19	0.12	
	H-atoms	0.13	0.10	0.05	
ρ_{bcp} (Covalent bond)	All atoms	0.21	0.31	0.15	
	Non-H atoms	0.20	0.33	0.18	
	H-atoms	0.23	0.29	0.10	
∇^2_{bcp}(Covalent bond)	All atoms	7.93	10.41	4.80	
	Non-H atoms	7.85	12.16	5.15	
	H-atoms	8.03	7.86	4.35	
ρ_{bcp} (H···Acceptor)		0.09	0.10	0.02	
∇^2_{bcp} (H···Acceptor)		1.18	0.84	0.40	

Table S11. Electrostatic potential surface quantities (Bohr Å^{-1}) of L-tyrosine

	$V^{+}_{s\ av.}$	$V^{-}_{s\ av.}$	Π
eMM_{exp}	0.182	-0.043	0.099
eMM_{theo}	0.196	-0.048	0.094
xMM_{exp}	0.181	-0.085	0.127

Table S12. Topological parameters of the covalent bonds of L-tyrosine.

Rij: BP length; d_1, d_2: distances between the BCP and each bonded atom, ρ_{bcp}: electron density and $\nabla^2\rho_{bcp}$: Laplacian at the BCP. For each covalent bond, the first, second and third lines refers to the eMM_{exp}, eMM_{theo} and xMM_{exp} models, respectively.

Bonds	*Rij* (Å)	d_1 (Å)	d_2 (Å)	ρ_{bcp} (e Å^{-3})	$\nabla^2\rho_{bcp}$ (e Å^{-5})
O1-C1	1.264	0.798	0.466	2.187	-7.816
	1.271	0.813	0.458	2.469	-25.777
	1.264	0.785	0.479	2.767	-34.557
O2-C1	1.251	0.791	0.460	2.219	-6.962
	1.256	0.818	0.438	2.531	-21.904
	1.252	0.794	0.458	2.828	-34.781
O3-C7	1.367	0.823	0.544	1.895	-4.212
	1.377	0.834	0.543	1.769	-6.537
	1.366	0.798	0.569	2.140	-15.586
N1-C2	1.504	0.931	0.573	1.426	-6.671
	1.498	0.854	0.644	1.510	-5
	1.490	0.839	0.651	1.667	-7.58
C1-C2	1.539	0.679	0.861	1.497	-4.864
	1.526	0.778	0.748	1.685	-11.238
	1.529	0.776	0.754	1.751	-11.579
C2-C3	1.538	0.751	0.788	1.719	-10.987
	1.544	0.819	0.725	1.498	-6.738
	1.544	0.802	0.742	1.551	-7.049
C3-C4	1.511	0.821	0.690	1.674	-10.403
	1.507	0.747	0.760	1.662	-10.247
	1.511	0.745	0.766	1.689	-9.249
C4-C5	1.399	0.647	0.753	1.935	-14.541
	1.395	0.722	0.673	2.055	-16.589
	1.401	0.691	0.709	2.161	-18.241
C4-C9	1.399	0.654	0.746	1.918	-14.415
	1.393	0.714	0.679	2.067	-17.078
	1.399	0.677	0.722	2.163	-16.692
C5-C6	1.391	0.693	0.698	2.083	-15.705
	1.384	0.679	0.705	2.105	-17.269
	1.393	0.686	0.707	2.209	-18.348
C6-C7	1.396	0.737	0.659	1.785	-8.054
	1.389	0.704	0.686	2.105	-17.744
	1.396	0.653	0.743	2.207	-18.558
C7-C8	1.399	0.659	0.741	1.775	-7.911
	1.391	0.679	0.713	2.070	-16.682
	1.397	0.718	0.679	2.188	-18.073
C8-C9	1.388	0.704	0.683	2.077	-15.909

	1.388	0.711	0.677	2.090	-17.612
	1.397	0.676	0.721	2.116	-15.147
O3-H9	1.011	0.805	0.206	1.966	-43.983
	0.992	0.791	0.201	2.072	-38.971
	0.980	0.766	0.214	2.349	-50.228
N1-H2	1.067	0.826	0.241	1.846	-25.4
	1.048	0.777	0.271	2.108	-36.152
	1.039	0.766	0.274	2.196	-34.718
N1-H3	1.064	0.809	0.255	1.935	-24.045
	1.042	0.773	0.269	2.130	-36.786
	1.040	0.771	0.270	2.124	-32.572
N1-H4	1.029	0.794	0.236	2.051	-28.969
	1.029	0.765	0.264	2.155	-36.385
	1.040	0.765	0.275	2.159	-31.76
C2-H1	1.114	0.738	0.376	1.704	-16.498
	1.089	0.728	0.361	1.869	-19.3
	1.099	0.719	0.380	1.909	-21.013
C3-H5	1.114	0.772	0.342	1.551	-11.866
	1.091	0.705	0.386	1.774	-15.757
	1.098	0.704	0.394	1.817	-16.194
C3-H6	1.108	0.786	0.322	1.491	-12.07
	1.092	0.702	0.390	1.821	-17.604
	1.097	0.702	0.396	1.859	-17.921
C5-H7	1.099	0.588	0.512	1.600	-10.059
	1.084	0.681	0.403	1.823	-17.163
	1.085	0.711	0.374	1.954	-22.588
C6-H8	1.089	0.588	0.502	1.611	-10.772
	1.081	0.708	0.373	1.861	-19.513
	1.085	0.701	0.384	1.903	-19.966
C8-H10	1.101	0.592	0.508	1.604	-10.275
	1.083	0.712	0.371	1.893	-21.451
	1.085	0.716	0.369	1.898	-19.371
C9-H11	1.098	0.579	0.519	1.569	-9.894
	1.083	0.705	0.378	1.801	-16.722
	1.085	0.721	0.364	1.875	-18.564

Table S13. Topological parameters of intermolecular interactions of L-tyrosine.

Rij: BP length; d_1, d_2: distances between the BCP and each bonded atom, ρ_{bcp}: electron density and $\nabla^2\rho_{bcp}$: Laplacian at the BCP. For each covalent bond, the first, second and third lines refers to the eMM_{exp}, eMM_{theo} and xMM_{exp} models, respectively.

Interactions	Symmetry codes	*Rij* (Å)	d_1 (Å)	d_2 (Å)	ρ_{bcp} (e Å^{-3})	$\nabla^2\rho_{bcp}$ (e Å^{-5})
O1···H2	65501	1.755	1.144	0.611	0.295	2.374
		1.763	1.150	0.613	0.311	1.601
		1.771	1.142	0.629	0.304	1.477
O1···H3	65603	1.818	1.162	0.656	0.275	2.246
		1.815	1.176	0.640	0.260	1.584
		1.830	1.176	0.655	0.248	1.595
O1···H6	65501	2.647	1.485	1.162	0.046	0.584
		2.690	1.552	1.138	0.037	0.595
		2.654	1.558	1.097	0.027	0.562
O2···H1	65603	2.225	1.268	0.957	0.156	1.191
		2.276	1.362	0.914	0.095	1.158
		2.219	1.329	0.890	0.110	1.153
O2···H9	56504	1.661	1.035	0.626	0.531	0.675
		1.676	1.117	0.559	0.309	3.368
		1.687	1.132	0.555	0.310	2.403
O3···H4	56504	2.080	1.303	0.777	0.152	1.996
		2.045	1.274	0.771	0.139	1.879
		2.085	1.310	0.775	0.094	1.995

Table S14. Single-crystal X-ray diffraction data and refinement parameters of L-tyrosine.

	L-Tyrosine
Chemical Formula	$C_9H_{11}NO_3$
Formula weight (g mol^{-1})	181.193
Temperature (K)	99.9(2)
Space group	$P2_12_12_1$
Unit cell *a*, *b*, *c* (Å)	5.8254(5), 6.8295(6), 21.1143(2)
Angles α, β, γ (°)	90, 90, 90
Volume (Å^3), Z	840.03(1), 4
Resolution (Å)	0.45
Density (g cm^{-3})	1.433
F(000)	384
μ (mm^{-1})	0.108
R_{int}, R_{merge} (%)	5.18, 2.96
Measured reflections	69371
Unique reflections	9595
Completeness (%)	99.9
Multiplicity	12.8
IAM refinement at 0.45 Å	
No. of reflection used obs [$I > 2\sigma(I)$]/ all	8950/ 9595
R_1 obs [$I > 2\sigma(I)$]/ all (%)	3.09/ 3.40
wR_1 obs [$I > 2\sigma(I)$]/ all (%)	7.93/ 8.08
GooF	1.072
$\Delta\rho_{max}$, $\Delta\rho_{min}$ (e Å^{-3})	0.45/-0.21
IAM refinement at 0.60 Å	
No. of reflection used obs [$I > 2\sigma(I)$]/ all	4165/ 4273
R_1 obs [$I > 2\sigma(I)$]/ all (%)	2.57/ 2.64
wR_1 obs [$I > 2\sigma(I)$]/ all (%)	7.36/ 4.42
GooF	1.046
$\Delta\rho_{max}$, $\Delta\rho_{min}$ (e Å^{-3})	0.42/-0.17

Table S15. Crystal data and multipole refinement parameters of xMM_{exp}

	L-alanine	**Urea**	**L-tyrosine**
Space group	$P2_12_12_1$	$P\text{-}42_1m$	$P2_12_12_1$
a (Å)	5.8033	5.5780	5.8254
b (Å)	5.9601	5.5780	6.8295
c (Å)	12.3012	4.6860	21.1143
α, β, γ (°)	90	90	90
Volume (Å^3)	425.477	145.80	840.02
Resolution (Å)	0.44	0.53	0.59
Completeness (%)	100	100	100
Multipole Refinement			
No. of reflection used obs [$I > 3\sigma(I)$]/ all	2831/2881	337/347	2383/2487
Constraints/ Restraints/ Parameters	0/7/152	0/2/49	0/11/338
R_1 obs [$I > 3\sigma(I)$]/ all (%)	1.05/1.09	0.87/0.92	0.99/1.09
wR_1 obs [$I > 3\sigma(I)$]/ all (%)	1.51/1.56	1.14/1.14	1.35/1.41
No. of reflection after symmetry averaging (obs [$I > 3\sigma(I)$]/all)	2831/2881	337/347	2383/2487
MR_1 obs [$I > 3\sigma(I)$]/ MR_1 all /MwR_1 all (%)	1.05/1.09/1.56	0.87/0.92/1.14	0.99/1.09/1.41
$GooF_{\text{obs/all}}$	0.87/0.89	0.98/0.97	0.73/0.74
$\Delta\rho_{max}$, $\Delta\rho_{min}$ (eÅ^{-3})	0.0616/-0.0877	0.0291/-0.0489	0.0478/-0.0533

Table S16. Crystal data and multipole refinement parameters of eMM_{theo}

	L-alanine	**Urea**	**L-tyrosine**
Space group	$P2_12_12_1$	$P\text{-}42_1m$	$P2_12_12_1$
a (Å)	5.7890	5.5780	5.8254
b (Å)	5.9387	5.5780	6.8295
c (Å)	12.2516	4.6860	21.1143
α, β, γ (°)	90	90	90
Volume (Å^3)	421.20	145.80	840.02
Resolution (Å)	0.44	0.53	0.59
Completeness (%)	100	100	100
Multipole Refinement			
No. of reflection used	5030	578	4312
Constraints/ Restraints/Parameters	0/0/64	0/0/24	0/0/161
R_1 all (%)	0.51	0.67	0.28
wR_1 all (%)	0.56	0.79	0.31
No. of reflection after symmetry averaging (all)	5030	578	4312
MR_1 all /MwR_1 all (%)	0.51/0.56	0.67/0.79	0.28/0.31
$GooF$ all	0.03	0.03	0.03
Residual potential Max./min. (eÅ^{-1})	0.0084/-0.0083	0.0017/-0.0023	0.0047/-0.0057

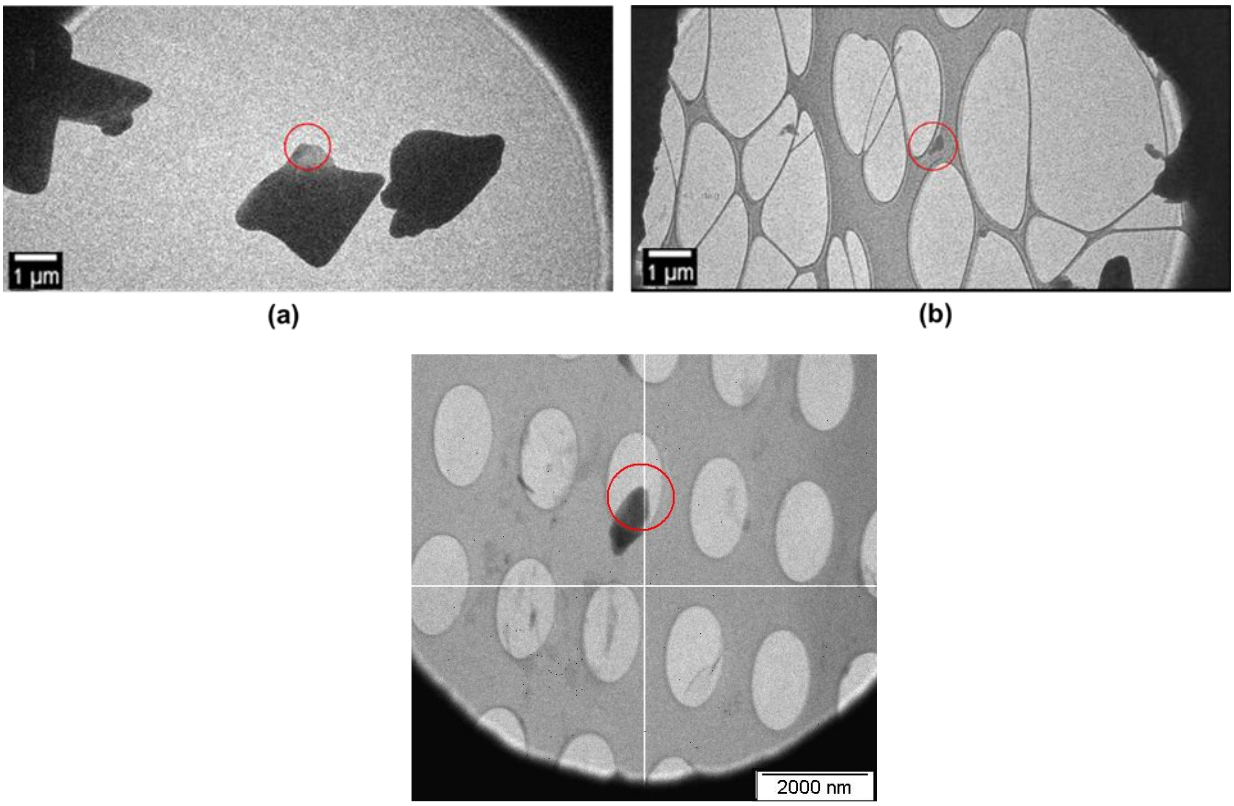

(a) **(b)** **(c)**

Fig. S1 | Images of crystals. (**a)** L-alanine, (**b)** Urea, (**c)** L-tyrosine.

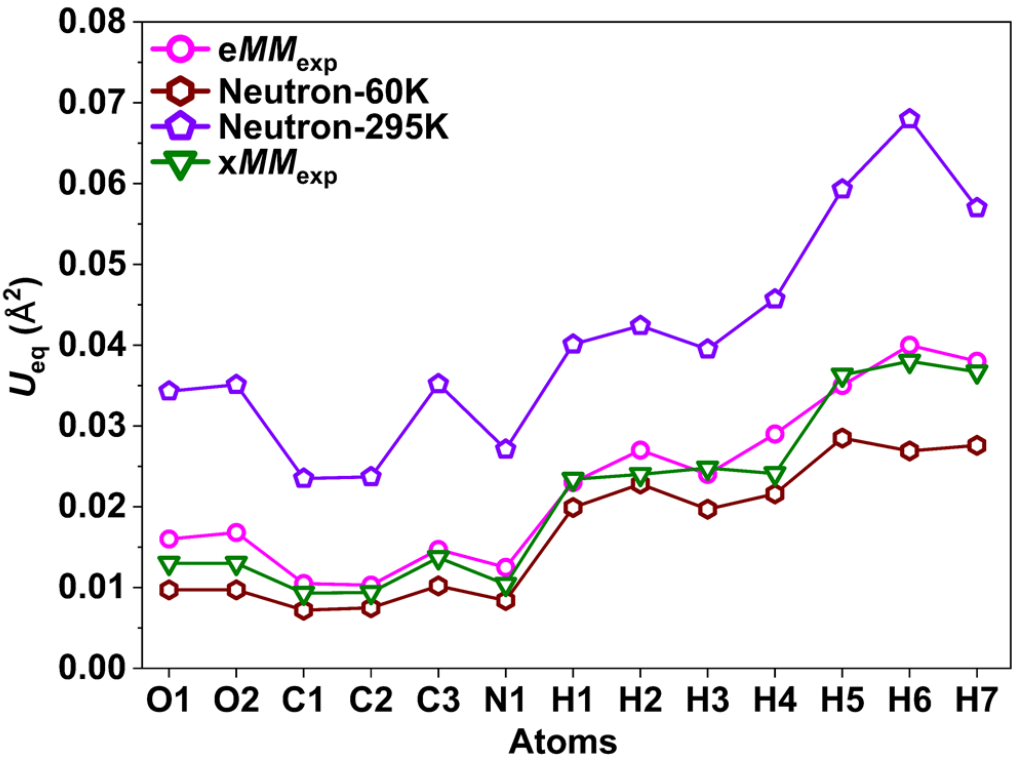

Fig. S2 | Comparison of U_{eq} of all atoms for L-alanine crystal. Ueq derived from the eMM$_{exp}$ are compared against results from xMM$_{exp}$ and neutron diffraction data at 60 K and 295 K.

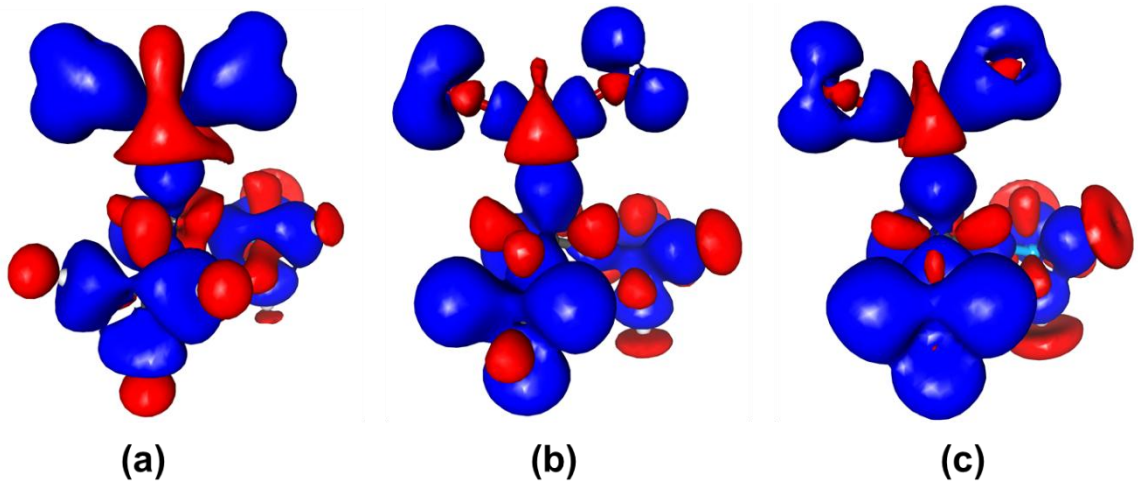

Fig. S3 | Comparison of 3D deformation density maps for L-alanine crystal. The maps are derived from (**a**) eMM$_{exp}$, (**b**) eMM$_{theo}$, and (**c**) xMM$_{exp}$ models. The positive (blue surface) and negative (red surface) of electron density isosurfaces are drawn at ± 0.1 e Å^{-3}.

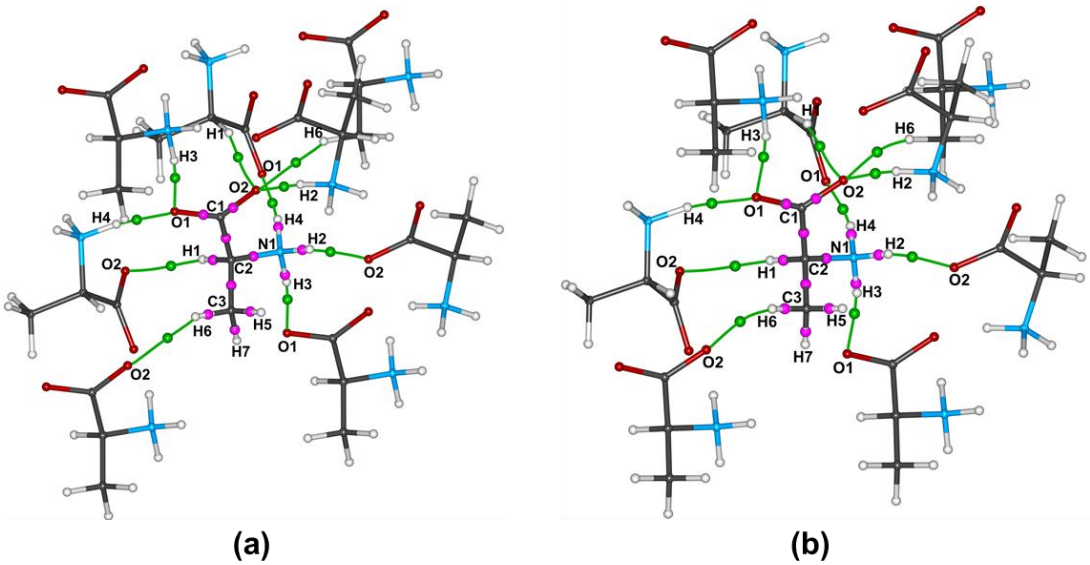

Fig. S4 | Description of chemical bonding for L-alanine crystal. Molgraph derived from (**a**) eMM_{theo} and (**b**) xMM_{exp} models. The central molecule is shown with its surrounding hydrogen-bonding network. Bond paths (green lines) and bond critical points (spheres) illustrate the covalent (magenta) and intermolecular (green) interactions.

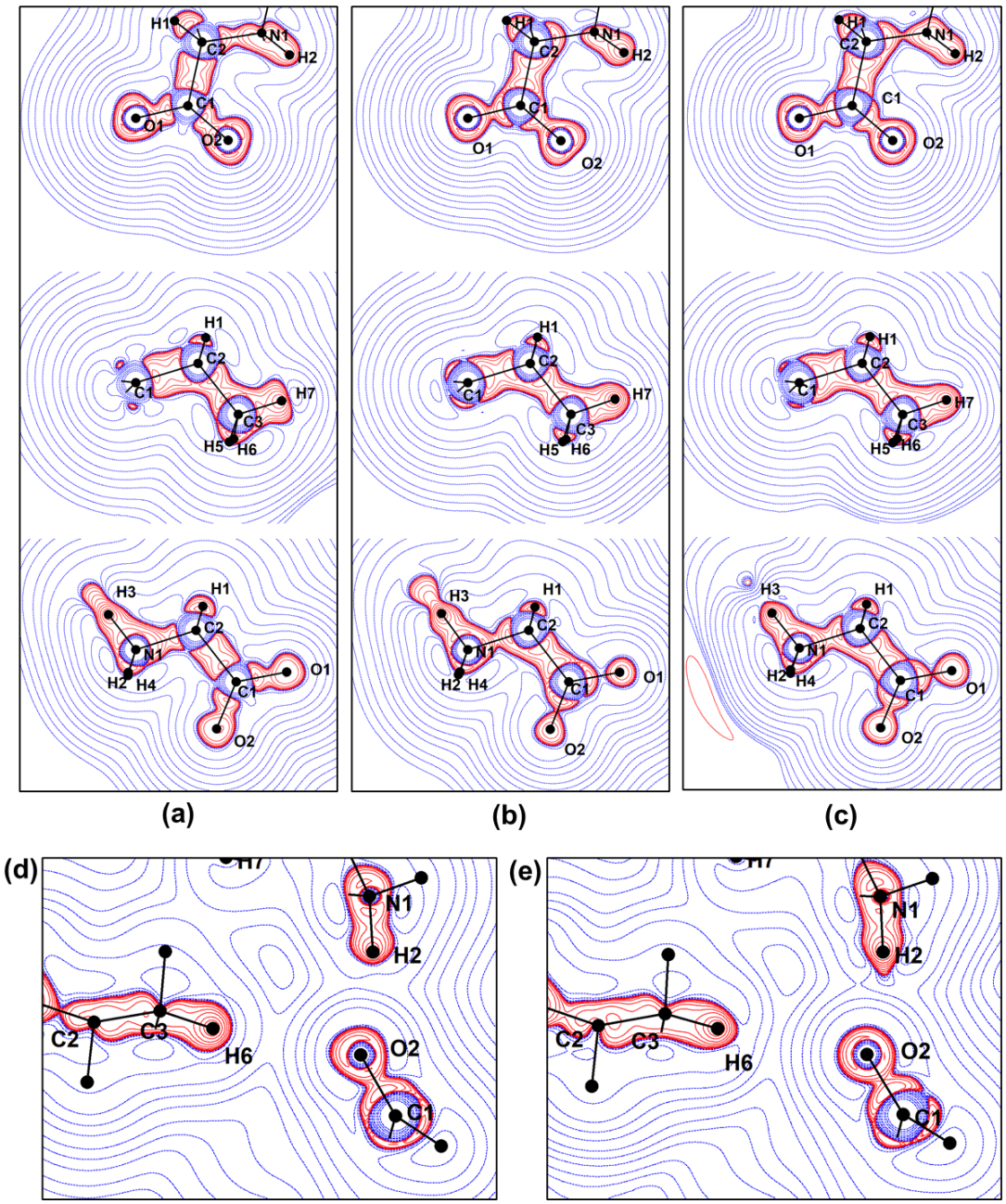

Fig. S5 | Laplacian maps of L-alanine crystal. Laplacian maps for covalent bond drawn in the molecular plane containing atoms O1, C1, O2 (top row), C1, C2, C3 (second row) and N1 C2 C1 (third row row) of (**a**) eMM_{exp}, (**b**) eMM_{theo}, and (**c**) xMM_{exp} models. Laplacian map for intermolecular interactions (bottom panle) of (d) eMM_{theo} and (e) xMM_{exp} models. Positive (blue dotted lines) and negative (red solid lines) contours are drawn at the level of ± 2 x 10^n, ± 4 x 10^n, ± 8 x 10^n (n = -3 to +2) e $Å^{-5}$.

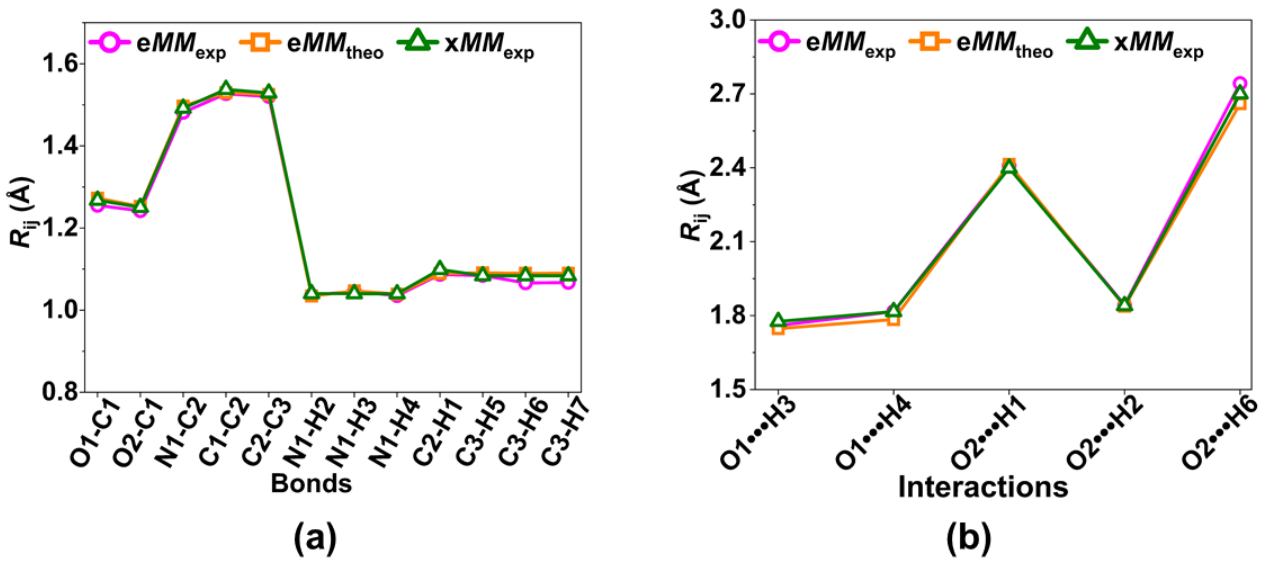

Fig. S6 | Comparison of bond path length (R_{ij}) in L-alanine crystal. R_{ij} for **(a)** covalent bonds and **(b)** intermolecular hydrogen bond interactions. Results from eMM_{exp}, eMM_{theo} and xMM_{exp} models.

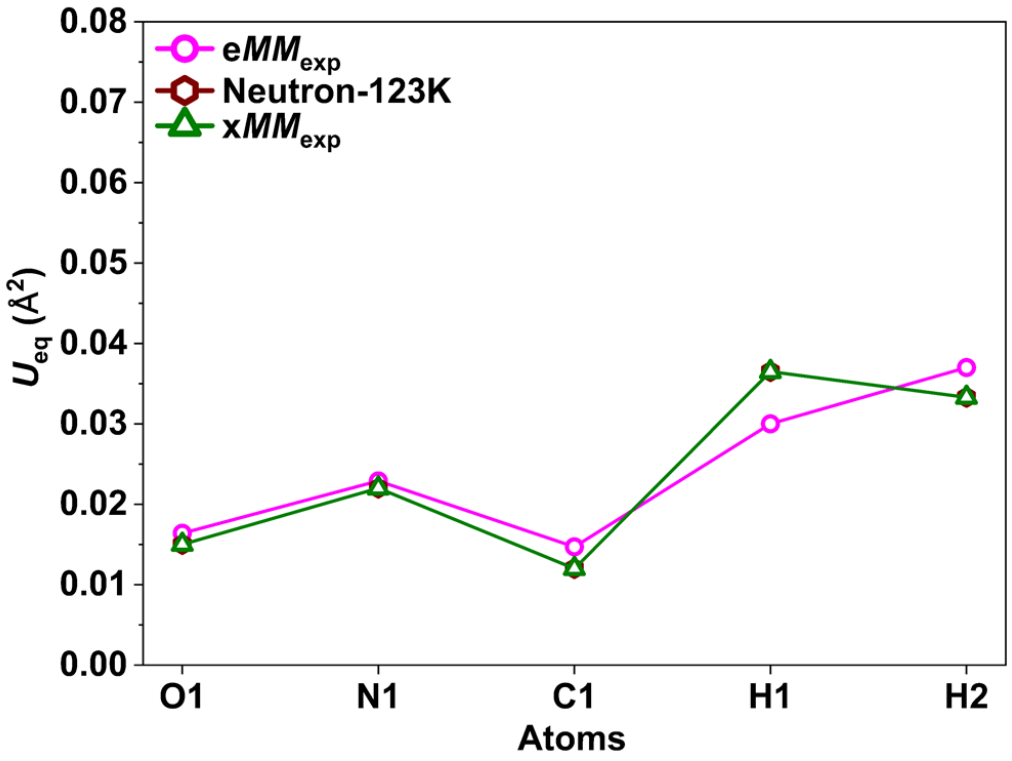

Fig. S7 | Comparison of U_{eq} of all atoms for urea crystal. U_{eq} derived from the eMM$_{exp}$ are compared against results from xMM$_{exp}$ and neutron diffraction data at 123 K.

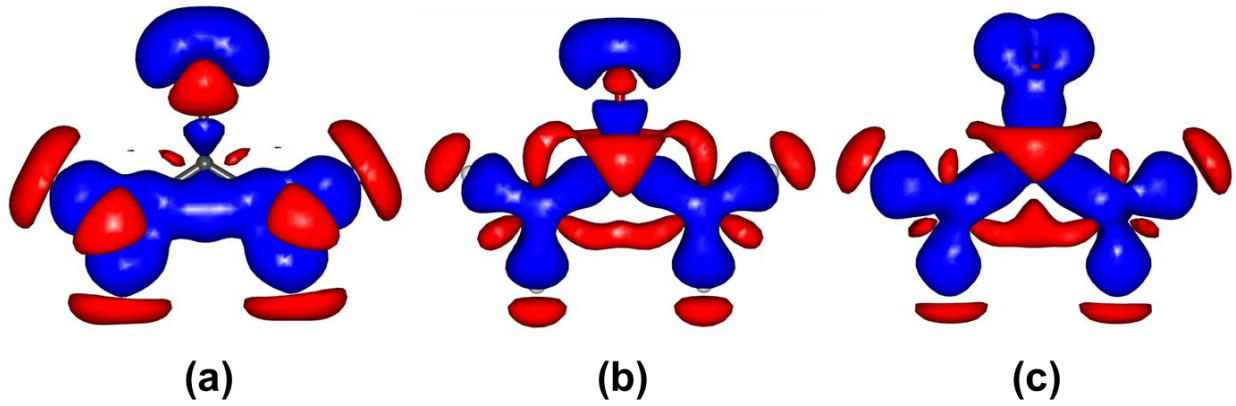

Fig. S8 | Comparison of 3D deformation density maps for urea crystal. The maps are derived from (**a**) eMM$_{exp}$, (**b**) eMM$_{theo}$, and (**c**) xMM$_{exp}$ models. The positive (blue surface) and negative (red surface) of electron density isosurfaces are drawn at ± 0.1 e Å^{-3}.

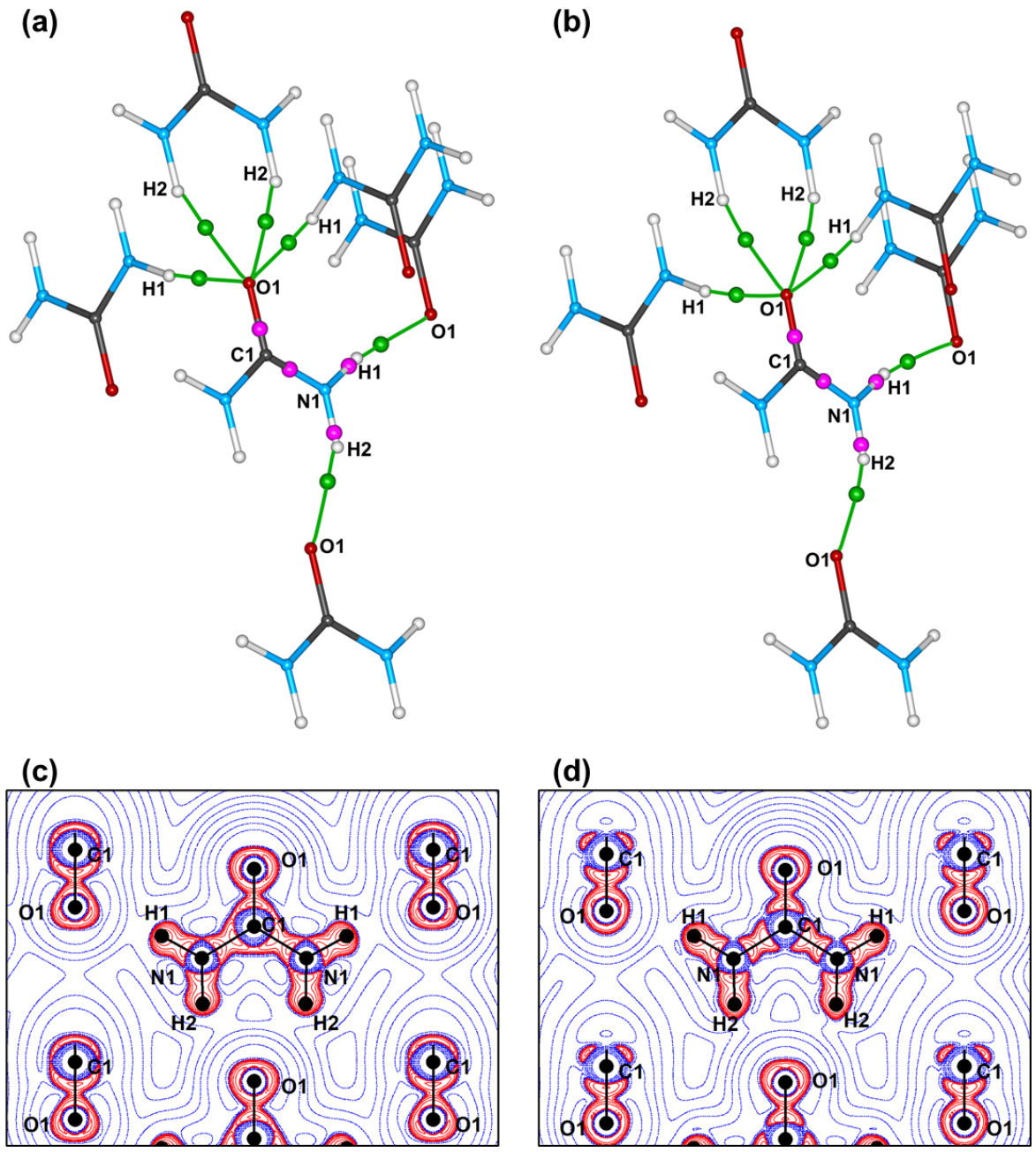

Fig. S9 | Description of chemical bonding and Laplacian maps for L-alanine crystal. Molecular graphs derived from (**a**) eMM_{theo} and (**b**) xMM_{exp} models. The central molecule is shown with its surrounding hydrogen-bonding network. Bond paths (green lines) and bond critical points (spheres) illustrate the covalent (magenta) and intermolecular (green) interactions. **c, d,** Laplacian maps for covalent bond and intermolecular interaction of **(c)** eMM_{theo} and **(d)** xMM_{exp} models. Positive (blue dotted lines) and negative (red solid lines) contours are drawn at the level of $\pm 2 \times 10^n$, $\pm 4 \times 10^n$, $\pm 8 \times 10^n$ (n = -3 to +2) e $Å^{-5}$.

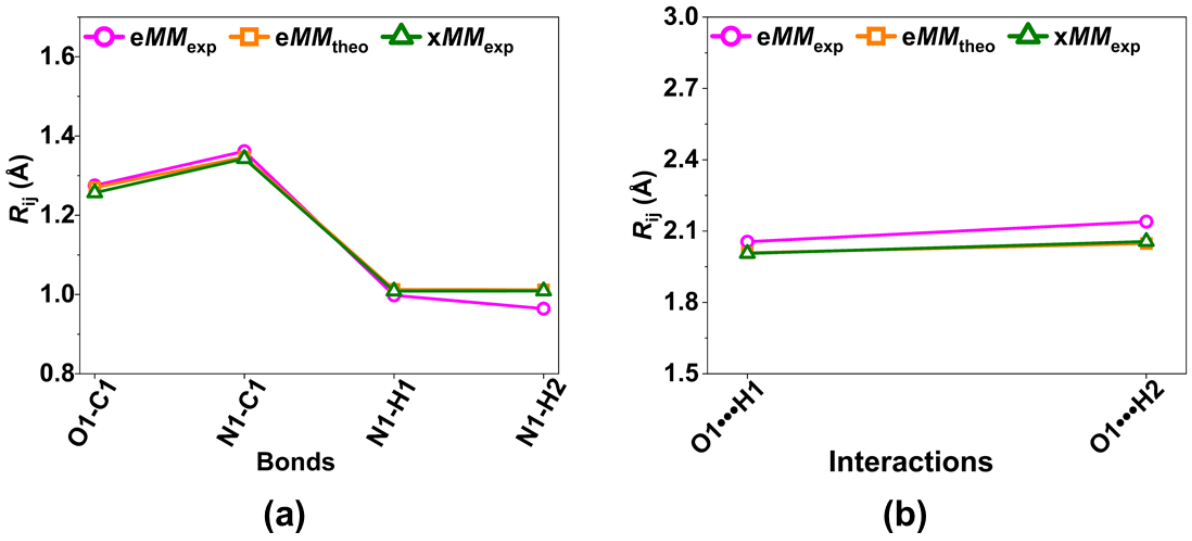

Fig. S10 | Comparison of bond path length (R_{ij}) in urea crystal. R_{ij} for **(a)** covalent bonds and **(b)** intermolecular hydrogen bond interactions. Results from eMM_{exp}, eMM_{theo} and xMM_{exp} models.

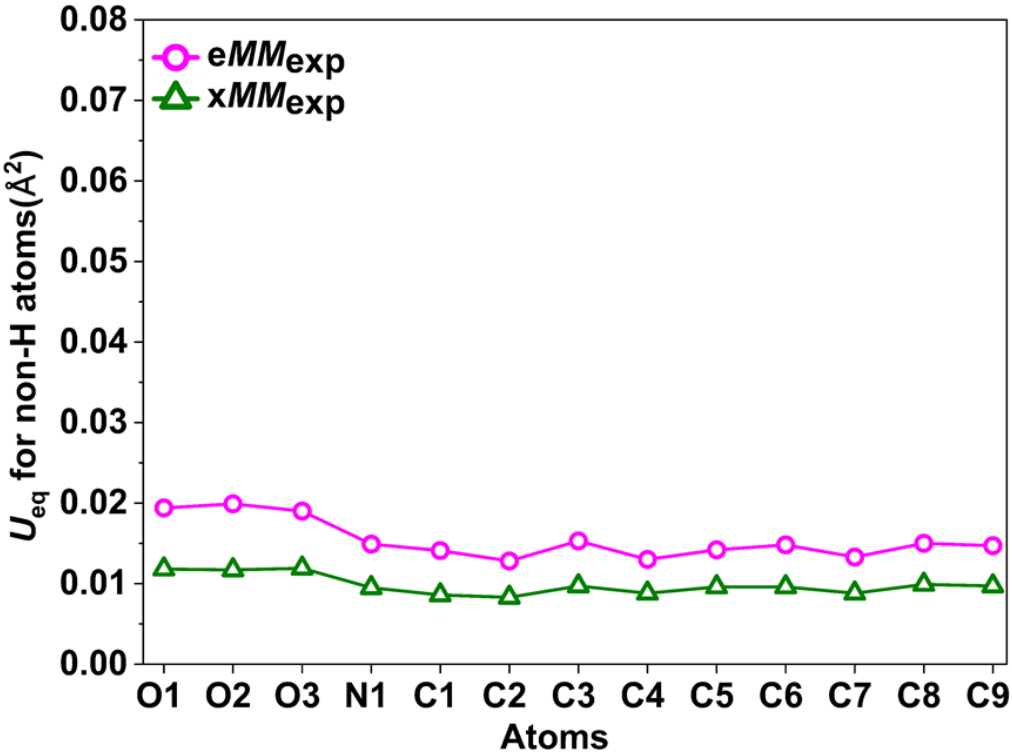

Fig. S11 | Comparison of U_{eq} of all atoms for L-tyrosine crystal. Ueq derived from the eMM_{exp} are compared against results from xMM_{exp}.

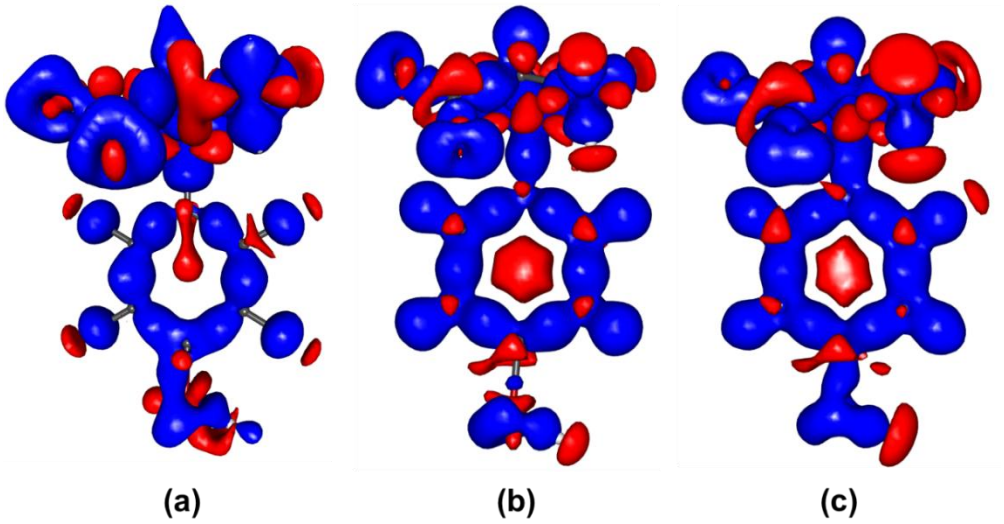

Fig. S12 | Comparison of 3D deformation density maps for L-tyrosine crystal. The maps are derived from (**a**) eMMexp, (**b**) eMMtheo, and (**c**) xMMexp models. The positive (blue surface) and negative (red surface) of electron density isosurfaces are drawn at ± 0.1 e $Å^{-3}$.

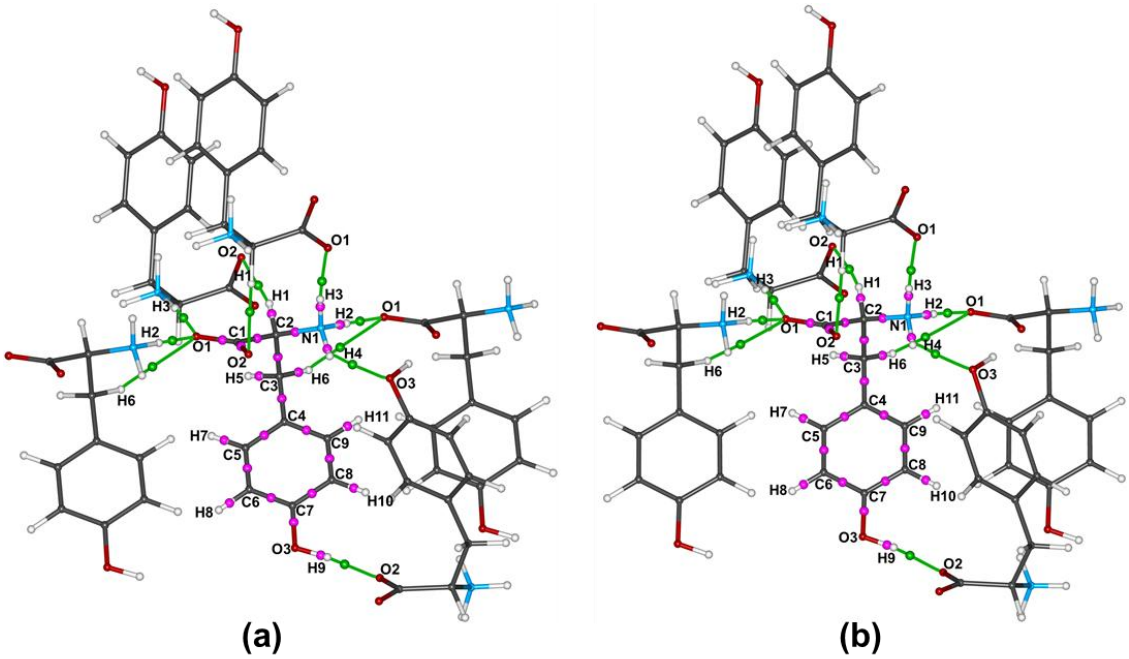

Fig. S13 | Description of chemical bonding for L-tyrosine crystal. Molgraph derived from (**a**) eMM_{theo} and (**b**) xMM_{exp} models. The central molecule is shown with its surrounding hydrogen-bonding network. Bond paths (green lines) and bond critical points (spheres) illustrate the covalent (magenta) and intermolecular (green) interactions.

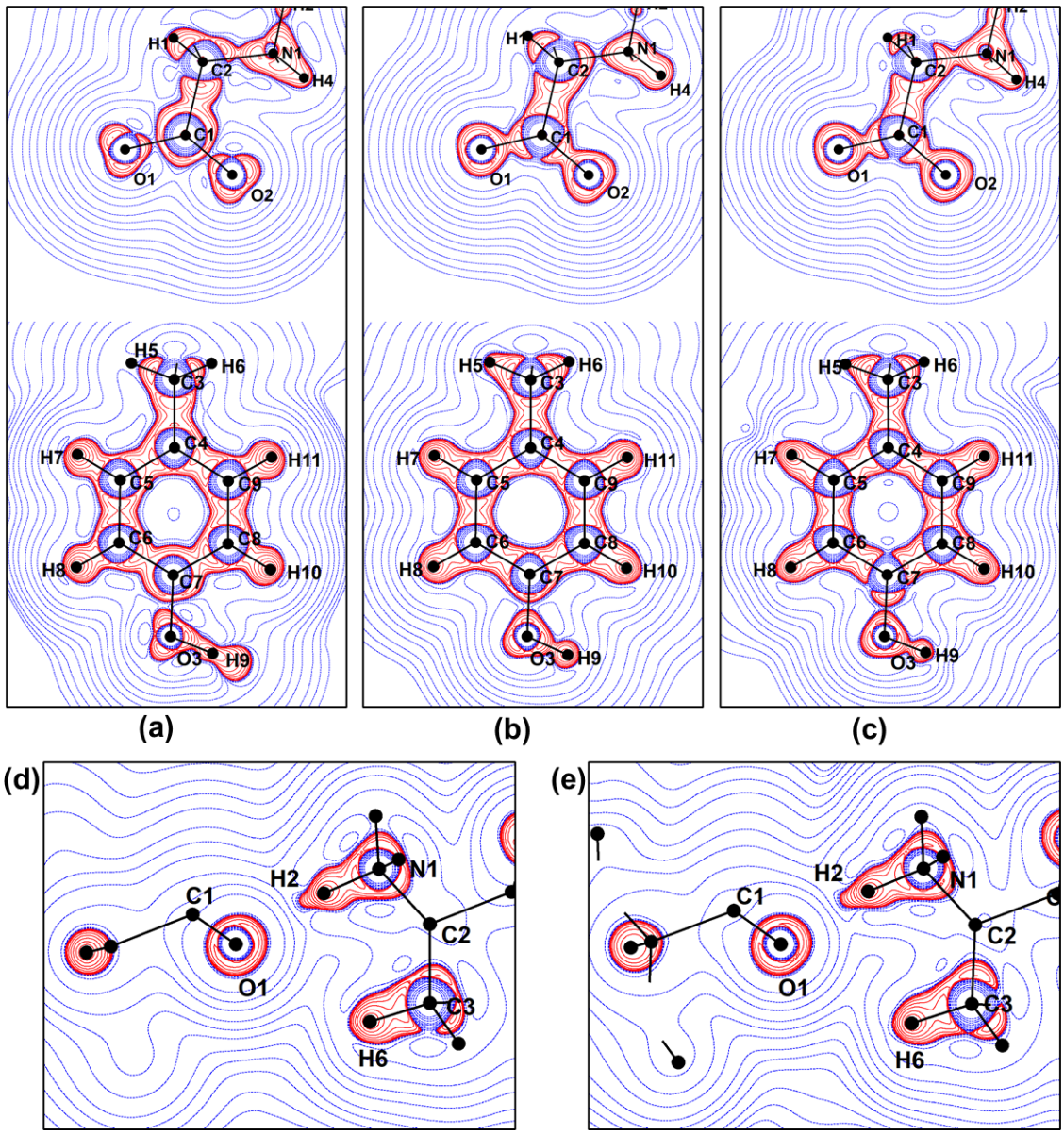

Fig. S14 | Laplacian maps of L-tyrosine crystal. Laplacian maps for covalent bond drawn in the molecular plane containing atoms O1, C1, O2 (top row) and C5, C4, C8 (second row) of (**a**) eMM_{exp}, (**b**) eMM_{theo}, and (**c**) xMM_{exp} models. Laplacian map for intermolecular interactions (bottom panel) of **(d)** eMM_{theo} and **(e)** xMM_{exp} models. Positive (blue dotted lines) and negative (red solid lines) contours are drawn at the level of $\pm 2 \times 10^n$, $\pm 4 \times 10^n$, $\pm 8 \times 10^n$ (n = -3 to +2) e $Å^{-5}$.

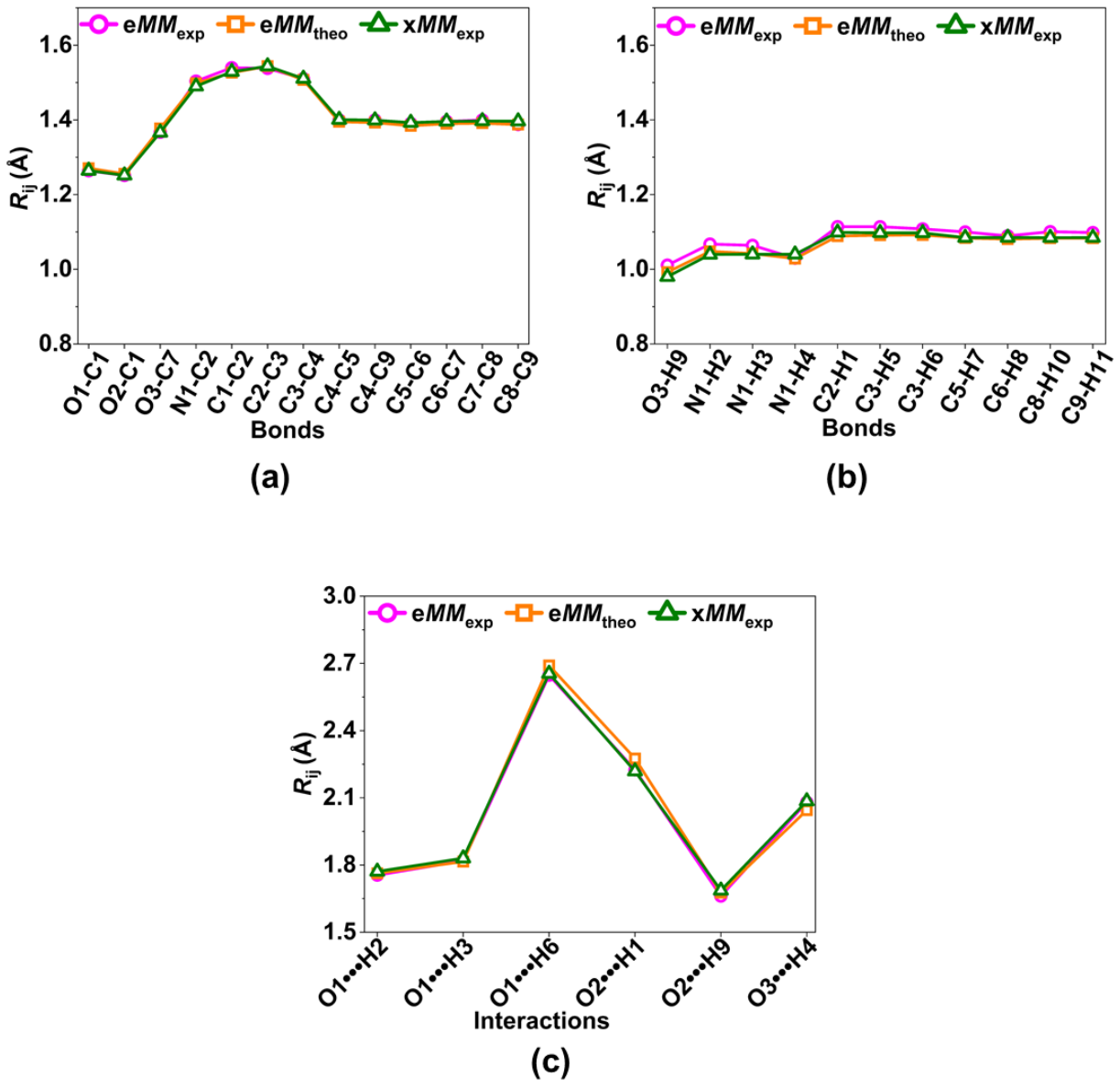

Fig. S15 | Comparison of bond path length (R_{ij}) in L-tyrosine crystal. R_{ij} for **(a)** non-H covalent bonds, **(b)** for H covalent bonds and **(c)** intermolecular hydrogen bond interactions. Results from eMM_{exp}, eMM_{theo} and xMM_{exp} models.

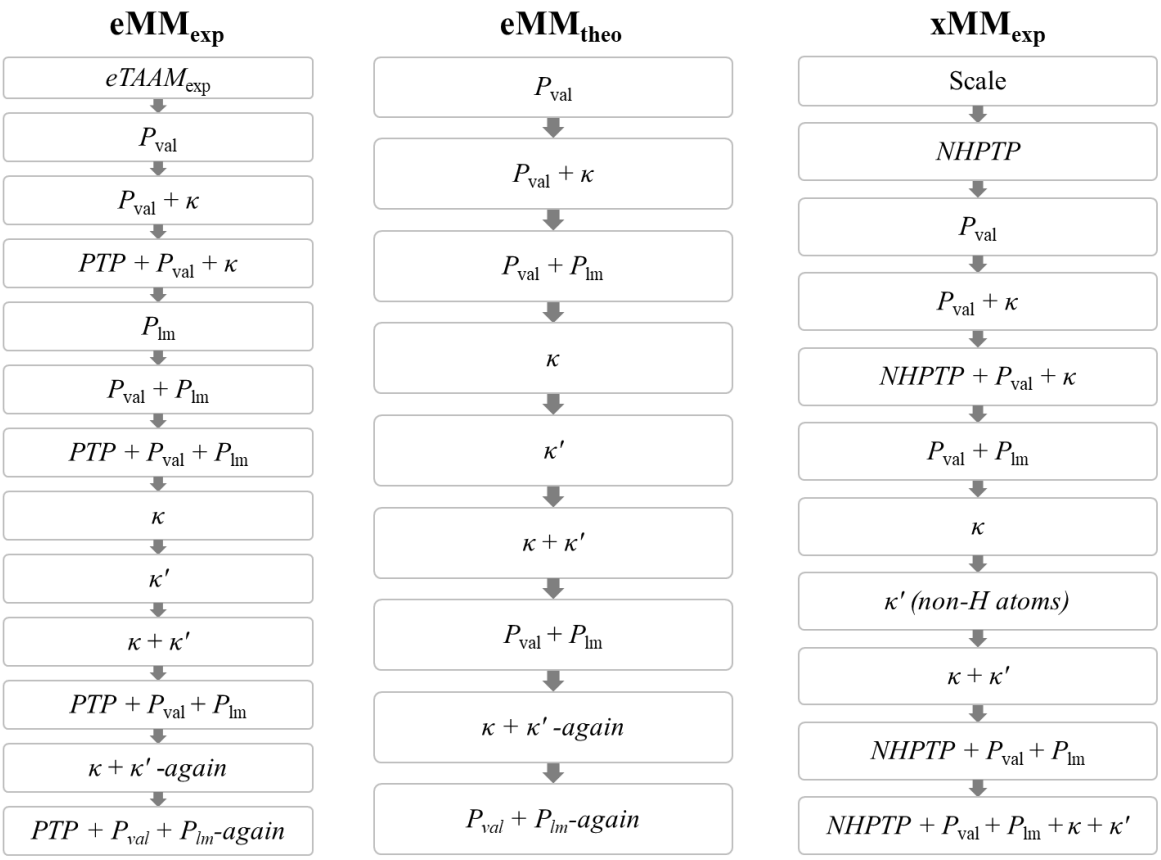

P_{val} - Valence electron population, P_{lm} - Multipolar population, κ & κ' -Expansion or contraction of the spherical and aspherical part, respectively, PTP- Atomic position and thermal parameters of all atoms and NHPTP- non-H atoms position and thermal parameters.

Fig. S16 | Flowchart of the iterative multipole model refinement strategy. The figure illustrates the detailed, step-by-step refinement strategy for eMM$_{exp}$, eMM$_{theo}$ and xMM$_{exp}$ models. For the multipole refinements of all three models, MATTS data bank was used as starting point. The κ and κ' parameters were refined individually for all the non-H atoms, for eMM$_{exp}$, eMM$_{theo}$ and xMM$_{exp}$ models. For H-atoms, κ and κ' parameters were assigned to be the same for the chemically equivalent types of atoms and refined for eMM$_{exp}$ and eMM$_{theo}$ and in case of xMM$_{exp}$, κ' parameters were constrained at the MATTS data bank values.

(0.14 x 0.064 x 0.05)

Fig. S17 | Single crystal of L-tyrosine for X-ray diffraction analysis. An optical microscope image showing the L-tyrosine single crystal mounted on a sample loop prior to X-ray data collection. The crystal size in mm is given in the parenthesis.

References

1. Blessing, R. H. An empirical correction for absorption anisotropy. *Acta Crystallogr. Sect. A Found. Crystallogr.* **51**, 33–38 (1995).

2. Farrugia, L. J. WinGX and ORTEP for Windows : an update. *J. Appl. Crystallogr.* **45**, 849–854 (2012).

3. Sheldrick, G. M. SHELXT – Integrated space-group and crystal-structure determination. *Acta Crystallogr. Sect. A Found. Adv.* **71**, 3–8 (2015).

4. Dolomanov, O. V., Bourhis, L. J., Gildea, R. J., Howard, J. A. K. & Puschmann, H. OLEX2 : a complete structure solution, refinement and analysis program. *J. Appl. Crystallogr.* **42**, 339–341 (2009).

5. Dovesi, R. *et al.* Quantum-mechanical condensed matter simulations with CRYSTAL. *WIREs Comput. Mol. Sci.* **8**, (2018).

6. Civalleri, B., Zicovich-Wilson, C. M., Valenzano, L. & Ugliengo, P. B3LYP augmented with an empirical dispersion term (B3LYP-D*) as applied to molecular crystals. *CrystEngComm* **10**, 405–410 (2008).

7. Peintinger, M. F., Oliveira, D. V. & Bredow, T. Consistent Gaussian basis sets of triple-zeta valence with polarization quality for solid-state calculations. *J. Comput. Chem.* **34**, 451–459 (2013).

8. Grimme, S. Semiempirical GGA-type density functional constructed with a long-range dispersion correction. *J. Comput. Chem.* **27**, 1787–1799 (2006).

9. Koritsanszky, T., Volkov, A., Farrugia, L. J., Mallinson, P. R., Macchi, P., Gatti, C. & Richter, T. *XD2024*. A computer program package for multipole refinement, topological analysis of charge densities and evaluation of intermolecular energies from experimental and theoretical structure factors.(2024).

10. *The scattering of electrons by atoms*. *Proceedings of the Royal Society of London. Series A, Containing Papers of a Mathematical and Physical Character* vol. 127 (1930).

11. Chodkiewicz, M. L. *et al.* DiSCaMB : a software library for aspherical atom model X-ray

scattering factor calculations with CPUs and GPUs. *J. Appl. Crystallogr.* **51**, 193–199 (2018).